Evidence for a Real-Time Singularity in Hydrodynamics from Time Series Analysis

R. B. Pelz* and Y. Gulak

Mechanical and Aerospace Enginnering, Rutgers, The State University of New Jersey, 98 Brett Road, Piscataway, New Jersey 08854-8058

(Received 29 April 1997)

The multiple-precision time series solution of the incompressible inviscid flow equations with the initial velocity field $u(x,y,z) = v(y,z,x) = w(z,x,y) = \sin x(\cos 3y \cos z - \cos y \cos 3z)$, has been computed to 32 terms and maximum wave number 99. Ratio test and Padé analyses indicate a real-time singularity in enstrophy $\Omega(t)$ with the form $(t_{\rm crit}^2 - t^2)^{-1}$ where $t_{\rm crit}\sqrt{\Omega(0)} \cong 4$. [S0031-9007(97)04859-X]

PACS numbers: 47.15.Ki, 02.30.Lt, 03.40.Gc

Whether the equations of inviscid, incompressible fluid flow have real-time blow-up solutions is a fundamental, unanswered question with important ramifications in fluid mechanics. Frisch [1] states that one of the central issues in the mathematical aspect of fully developed turbulence is the existence of singularities, whose form would, for instance, influence scaling properties. Why typical turbulent structures have severely depleted nonlinearity is a question that may be answered by first understanding singular flows which possess no depletion. A singularity may also be a release mechanism for flows with topologically confined vortex lines, and may be a source of focusing applications.

Mathematical discussions on the problem of global regularity of solutions of the Euler and Navier-Stokes equations can be found in the recent books by Doering and Gibbon [2], Temam [3], Marchioro and Pulvirenti [4] and references therein. Roughly speaking, the upper bound on the growth of the spatial supremum of vorticity, which occurs when strain rate is a function of vorticity, is t^{-1}. More precisely, for a real-time singularity to occur at $t_{\rm crit}$, the time integral of this quantity must become infinite at this time or before [5]. There have been computational works (too numerous to mention here) that showed evidence of singular behavior of the vorticity supremum, but because this is one of the most challenging numerical analysis problems, results to date are only suggestive.

Numerical evidence from one such pseudospectral simulation of the incompressible equations of fluid flow with highly symmetric initial conditions [6] suggests that a six-vortex dipole structure which is collapsing towards the origin leads to a real-time singularity. A symmetric vortex filament system [7] which is modeled after this structure, produces an attracting, locally self-similar collapse solution. While the two results are consistent, each of the analyses has its weaknesses. The pseudospectral simulations suffer from loss of accuracy at late times, and the 1-*d* filament model does not have proper core dynamics. Further investigations of this high symmetric flow are necessary. The purpose of this paper is to present findings from a different approach, that of a multiprecision, extended-time series analysis of the same highly symmetric flow.

We use an approach similar to that of Taylor and Green [8] by assuming a perturbation series in time for the velocity

$$\mathbf{V} = \sum_{p=0}^{\infty} \mathbf{V}_p t^p. \tag{1}$$

Plugging the series into the Euler equations,

$$\frac{\partial \mathbf{V}}{\partial t} + \mathbf{V} \cdot \nabla \mathbf{V} = -\nabla P, \qquad \nabla \cdot \mathbf{V} = 0, \tag{2}$$

where P is the pressure, $\mathbf{V}_p$ is found through a recursion of the terms $\{\mathbf{V}_q\}, q = 0, 1, \ldots, p-1$. If the initial field $\mathbf{V}_0$ in a three-dimensional periodic domain has a Fourier series decomposition and rational coefficients, so do the subsequent terms, and the recursion can be formed exactly.

From the velocity terms $\{\mathbf{V}_p\}, p = 0, 1, \ldots, 32$, the finite-term, time series for enstrophy is computed. This Maclaurin series is even due to time reversal and diverges as t approaches the radial value of the closest singularity. Analysis of the divergent series indicates that this closest singularity is near the imaginary axis and shields the detection of other possible singularities at larger distances from $t = 0$ even though the series contains information on them.

We use two methods to rerepresent the divergent, finite-term enstrophy series and investigate the singularities beyond the closest. The first is the Padé summation technique, which allows an analytic continuation of the series beyond the first singularity. The other is the Cauchy ratio test of the series in which the closest singularity has been mapped far from the origin.

Because of the nonlinear nature of the Padé summation technique, there is no general convergence proof. Even if there were, it would be of limited value since the series generated here has only a finite number of terms. Nevertheless, the Padé summation technique has been used quite successfully to improve convergence of finite term,

 0031-9007/97/79(25)/4998(4)$10.00

divergence series in many physical problems [9]. Known caveats in usage are errors stemming from insufficient precision of the series coefficients, and the intermittent behavior of nearly coincident zero/pole "defects," both of which we shall address in the paper.

From these rerepresentation techniques of the enstrophy, we find a simple, isolated pole on the real-time axis independent of precision and degree of approximation. This result is not a proof of the existence of a hydrodynamic blowup solution, since it is deduced from a finite-term representation. It does, however, provide another indication (along with [6,7]) of singular behavior in highly symmetric flows and provides a direction for further analysis.

This technique was used over ten years ago for investigations of the Taylor-Green vortex (TG), but attempts to isolate singularities were inconclusive. Series to orders 4, 8, 44, and 80 were found in Refs. [8,10–12], respectively. The investigations in the first two references did not reveal singular behavior. In the analyses of Morf, Orszag, and Frisch and Brachet *et al.* [11,12], Padé resummation of the series indicated that a real-time singularity in the enstrophy exists, although subsequent pseudospectral Euler simulations [13] found no evidence of a singularity.

The initial flow we examine in this paper, which is given in the abstract, is similar in nature to the Taylor-Green vortex. The TG symmetries in each direction, 2π translational, reflectional about planes $n\pi$, and π rotational about the lines $(n+1)\pi/2$ $(n = 0, 1, \ldots)$, are preserved by the Euler equations. For the present initial field, which is termed the high-symmetry initial condition, a $\pi/2$ rotational symmetry about the same lines is used. From these symmetries, the cyclic permutation of velocity $u(x, y, z) = v(y, z, x) = w(z, x, y)$ can be derived, which can also be seen as a $2\pi/3$ rotational symmetry about the line $x = y = z$. Kida [14] was the first to use these symmetries to gain higher resolution in turbulence simulations.

The cyclic permutation plays a critical role in the dynamics. It provides a way for the positive strain rate produced by a vortex dipole near the origin to be directed back on the dipole as axial stretching, thus linking vorticity and strain rate and preventing depletion of the nonlinearity. Using all the symmetries also greatly simplifies the series representation and recursion operation.

We started to generate the series with the computer algebra package FORM [15], a program that can manipulate very large formulas. Eleven exact terms were computed before FORM's integer-length limit of 480 digits was exceeded. We continued the analysis with the GMP [16] and MPFUN [17] extended precision packages in C and Fortran. Series were found for a number of precisions including exact (16 terms), 154 (28 terms), 77 (32 terms), 51 (26 terms) and 29 digits (16 terms). Careful attention was paid to truncation errors and precision. Because of truncation error, the precision decreased by about one digit every three terms. With the exponent range of the Fourier coefficients increasing by about five places every two terms, the smallest magnitude coefficients of the sixteenth term could not be distinguished from roundoff error in the 29-digit series. This occurred at the 26th term for the 51-digit series.

TABLE I. Coefficients of the enstrophy series A_n as given in Eq. (4) for the 77-digit series (rounded to 40 digits).

n	A_n
0	33/8
1	2123/480
2	3.8481656583957343138134098586075987205 93
3	−5.5407365228517733274997099703056709197 51
4	14.1049334733013979799083718930358214526 3
5	−31.6614461311672586250735049013820299398 7
6	65.9778196614061568619036838319992464944 5
7	−123.4312214664711517008338131705589843103
8	201.1211240149986858663566058334491631555
9	−258.6551464165619910095346398235215226700
10	130.8767678216434162498915121397318885203
11	732.9148587160793136299612084865127132055
12	−4025.7916434067890370687280381052664871 80
13	14752.5519214136455413486225479098944104 6
14	−47427.5160188536262410160975779720584049 2
15	143790.4245136551444888147675454747723734
16	−423523.1014514189545277106457927681229459

The enstrophy is defined as

$$\Omega \equiv \frac{1}{2\mathrm{Vol}} \int \omega^2 \, d\mathbf{x}\,, \tag{3}$$

where the vorticity is $\boldsymbol{\omega} = \nabla \times \mathbf{V}$. A series approximation to the enstrophy was computed from the velocity series and has the form

$$\Omega_N = \sum_{n=0}^{N} A_n t^{2n}. \tag{4}$$

To produce the nth term of the enstrophy series, $2n$ terms of the velocity series are required.

In Table I the terms of the enstrophy expansion are given for the 77-digit series. The gross behavior of the coefficients suggests that there is a singularity at a polar angle that is close to π in t^2 and within the unit disk.

The series for enstrophy was recast in algebraic (Padé and generalized Padé) approximates using the Gfun Maple package [18]. The Jth algebraic approximate to Ω_N has the form

$$\sum_{j=0}^{J} R_j(t) \Omega_N^j(t) = 0\,, \tag{5}$$

where each $R_j(t)$ is a r_jth order polynomial in t with the constraint $\sum_{j=0}^{J} r_j = 2N$. These approximates are represented by $[r_0, r_1, \ldots, r_J]$. A Padé approximate is a linear $(J = 1)$ approximate of the form $R_1(t)\Omega_N(t) + R_0(t) = 0$. If the orders of R_1 and R_0 are r_1 and r_0, respectively, then $r_1 + r_0 = 2N$ and the representation is $[r_0, r_1]$. Likewise, a quadratic approximate $[r_0, r_1, r_2]$ has the form $R_2(t)\Omega_N^2(t) + R_1(t)\Omega_N(t) + R_0(t) = 0$ with $r_2 + r_1 + r_0 = 2N$.

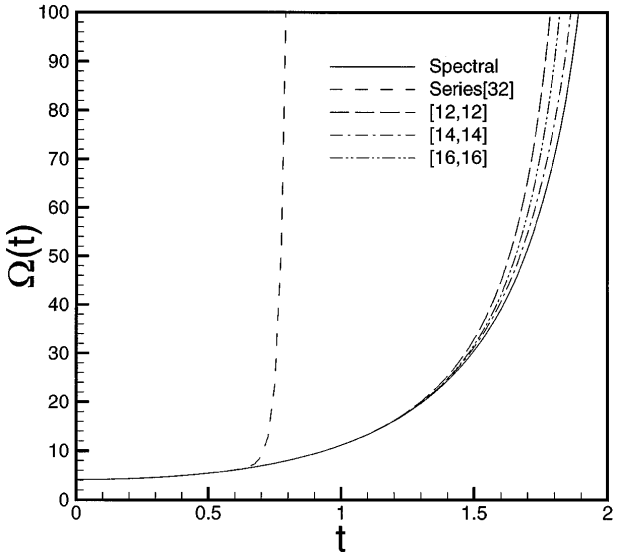

FIG. 1. Plot of approximates to enstrophy vs real time for the 1200^3 pseudospectral simulations (solid), the 32-term Taylor series (dashed), and some Padé approximates.

In Fig. 1, we plot enstrophy versus real time for the Euler pseudospectral computation with effective resolution of 1200^3 (solid) [19], the 32-term time series (dashed), and various Padé approximates. The convergence of the series is clearly affected by singularities off the real axis, whereas the curves from the approximates are all much closer together and to the simulation curve. When $t > 1.3$, the simulations show that the width of the analyticity strip is less than one mesh size, suggesting that the simulations are becoming less accurate with time. At this time, the approximate and simulation curves start to diverge.

Table II shows the location of all the poles of the algebraic approximates. An isolated real singularity is consistently found at a time of 2.04 ± 0.09. This critical time was found to be a linear function of $\Omega(0)^{-1/2}$. The scale factor is close to a value of four: $t_{\text{crit}} \approx 4/\sqrt{\Omega(0)} = 1.96946\ldots$.

TABLE II. Poles of the algebraic approximates of the enstrophy series rounded to 6 digits (first quadrant only).

Approx.	Real-time poles	Complex-time poles
[4, 4]	1.99252	$0.64806i$
[6, 6]	1.95039	$0.62177i, 0.53302i$
[4, 4, 4, 4]	1.97538	$0.66526i$
[8, 8]	1.99395	$0.70849i, 0.18284 + 0.642596i$
[6, 6, 6]	1.97309	$0.15379 + 0.65557i$
[10, 10]	1.97008	$0.08008 + 0.65910i, 0.35246 + 0.64475i$
[8, 8, 8]	1.97157	$0.15263 + 0.67684i, 0.38615i$
[6, 6, 6, 6]	1.97212	$0.01001 + 0.58319i$
[12, 12]	1.96971	$0.354241 + 0.646929i, 0.285261i$ $0.08071026 + 0.659760i$
[14, 14]	2.12851	$0.44467 + 0.85129i, 0.08026 + 0.75467i$ $2.25403i, 0.58988i$
[16, 16]	2.02046	$0.421803 + 0.847303i$ $0.080899 + 0.749964i$ $1.20714 + 1.15242i, .589432i$

TABLE III. Zeros of some Padé approximates of the enstrophy series (first quadrant only).

Approx.	Zeros in t
[8, 8]	$0.18015 + 0.63024i, 0.15624 + 0.81971i$
[10, 10]	$0.35556 + 0.64597i, 0.12058 + 0.67139i, 0.90476i$
[12, 12]	$0.35749 + 0.64804i, 0.12157 + 0.67114i$ $0.90730i, 0.28526i$
[14, 14]	$0.62642 + 1.2962i, 0.42583 + 0.79596i$ $0.15668 + 0.67856i, 0.58847i$
[16, 16]	$0.41844 + 0.79218i, 0.15637 + 0.67855i$ $1.0715 + 1.1515i, 0.58806i, \pm 1.6034i$

As can be seen in the third column of Table II, the approximates predict a range of locations of the complex-time poles which changes with order. Some of the approximates have nearly coincident poles and zeros. This results in near cancellation and is called a defect. To understand this behavior, the locations of the zeros of some approximates are given in Table III. Plotted in Fig. 2 are the locations of all the poles (outlined) and defects (filled) for Padé approximates [12, 12] (squares), [14, 14] (diamonds), and [16, 16] (circles) in the complex time plane. Baker and Grave-Morris [9] state that defects are transient with order, effectively fictitious, and to be expected with Padé approximates and that true singularities will have a behavior which is stable with order. Neglecting the defects, the field becomes less cluttered.

To analyze the form of the real-time singularity at $t = t_{\text{crit}}$, the origin-preserving bilinear transformation

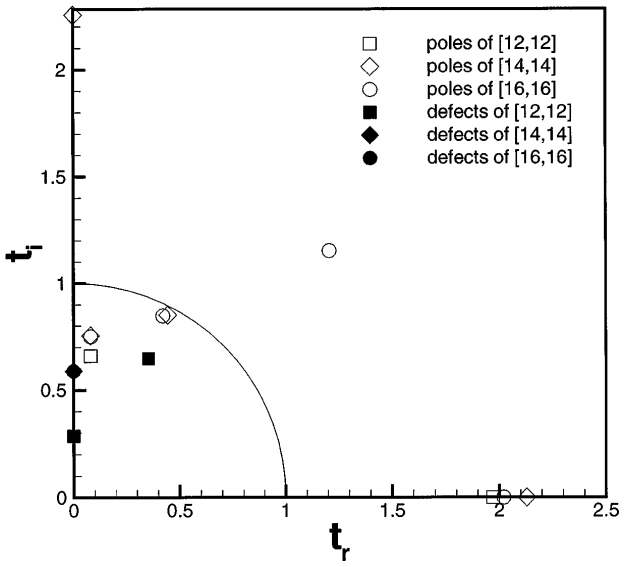

FIG. 2. Plot of locations of poles (outlined) and defects (filled), nearly coincident zeros and poles, of enstrophy in the complex time plane for the Padé approximates [12, 12] (squares), [14, 14] (diamonds), and [16, 162] (circles).

TABLE IV. Table of the ratios B_{n-1}/B_n, as defined in Eq. (7), which are estimates of s_{crit}. Also listed are estimates of t_{crit} and biased estimates of the order of the singularity γ. The Euler transformation of enstrophy is given in Eq. (6) with $a = 0.575$.

n	B_{n-1}/B_n	Estimates of t_{crit}	Estimates of $-\gamma$
2	0.77660203341358	1.0720807511772	−1.3787066405075
3	0.89521496878252	1.6806678361270	−1.0953041643588
4	0.91767461012944	1.9197527776524	−1.0260641266995
5	0.91958055790291	1.9443847539528	−1.0221494953234
6	0.91999644219909	1.9498727424175	−1.0238550797986
7	0.92125444120982	1.9667293882922	−1.0182342244159
8	0.92246431359793	1.9833155354673	−1.0103192575869
9	0.92297901395155	1.9904864281945	−1.0065838301311
10	0.92277837889223	1.9876828590919	−1.0094912070339
11	0.92218150824131	1.9794049170708	−1.0175666999606
12	0.92156334967305	1.9709287412692	−1.0272257869278
13	0.92120139253489	1.9660106506706	−1.0346141329532
14	0.92123125807386	1.9664152014589	−1.0368216819137
15	0.92166468738083	1.9723115970781	−1.0323792307986
16	0.92243129609908	1.9828578996699	−1.0212119577879

$$s = \frac{t^2}{t^2 + a^2} \tag{6}$$

is used to map the real-time singularity closest to the origin. The constant a is close to the value of the imaginary part of the complex-time singularities. A new series for enstrophy is created

$$\Omega_N(t) = \hat{\Omega}_N(s) = \sum_{n=0}^{N} B_n s^n. \tag{7}$$

If enstrophy has the form $\Omega = (t_{\text{crit}} - t)^{-\gamma} h(t)$ where $h(t)$ is analytic near t_{crit}, then the ratios B_n/B_{n-1} approach a value equal to the inverse of the radius of convergence, $1/s_{\text{crit}}$, and a slope of $\gamma - 1$ as $n \to \infty$. The values for B_{n-1}/B_n, and estimates of t_{crit} and γ for each n are given in Table IV for $a = 0.575$. The estimated values for t_{crit} are close to those of the approximates, and the estimated values for γ, biased by an assumed critical time of 2, are close to 1 indicating a simple pole.

A simple pole behavior is also found using D log Padé analysis. The $[8, 8]$ Padé approximate of $(s_{\text{crit}} - s)\frac{d}{ds} \ln \Omega_N(s)$ evaluated at $s = s_{\text{crit}} = 0.92$ gives a biased value of the pole order of 1.015 for $a = 0.6$.

Results of Kerr [20] indicate a $\ln(t_{\text{crit}} - t)$ behavior for enstrophy in the anti-parallel vortex tube problem. A $(t_{\text{crit}} - t)^{-1/2}$ behavior was found for enstrophy in the symmetry vortex filament model [7]. That a singularity stronger than is predicted by the filament model is found here may be due to the fact that two more symmetries are enforced in the series solution.

How do the series results of the high-symmetry flow compare to those of the Taylor-Green vortex [11,12]? The number of nonzero modes of the pth term, $3(p + 1)/2$ $(p = 32)$, is larger than in the TG studies, $(p + 3)/2$ $(p = 80)$. The singularities detected in the TG flow are relatively far away from the origin and the distribution is complicated (many singularities were found with approximately the same radii and with time arguments of $|\pi/8|$ or less). The real-time singularity in the high-symmetry flow is closer to the origin, away from zeros and other poles, and easy to isolate by Euler transformation.

We should like to thank S. Orzsag for suggesting this analysis, O. Boratav for sharing data from the pseudo-spectral simulations, and J. Greene for useful suggestions. Computations were done on the C90 at the Pittsburgh Supercomputer Center, the SP2 at the Cornell Theory Center, and computers at the CAIP Center at Rutgers.

*Electronic address: pelz@jove.rutgers.edu

[1] U. Frisch, *Turbulence* (Cambridge University Press, Cambridge, 1995).
[2] C. R. Doering and J. D. Gibbon, *Applied Analysis of the Navier-Stokes Equations* (Cambridge University Press, Cambridge, 1995).
[3] R. Temam, *Navier-Stokes Equations and Nonlinear Functional Analysis* (SIAM, Philadelphia, 1995).
[4] C. Marchioro and M. Pulvirenti, *The Mathematical Theory of Incompressible Nonviscous Fluids* (Springer, New York, 1991).
[5] J. T. Beale, T. Kato, and A. Majda, Commun. Math. Phys. **94**, 61 (1985).
[6] O. N. Boratav and R. B. Pelz, Phys. Fluids **6**, 2757 (1994).
[7] R. B. Pelz, Phys. Rev. E **55**, 1617 (1997).
[8] G. I. Taylor and A. E. Green, Proc. R. Soc. London A **158**, 499 (1937).
[9] G. A. Baker and P. Grave-Morris, *Padé Approximates, Part I: Basic Theory* (Addison-Wesley, Reading, 1981).
[10] M. Van Dyke, SIAM J. Appl. Math. **28** 720 (1975).
[11] R. H. Morf, S. A. Orszag, and U. Frisch, Phys. Rev. Lett. **44**, 572 (1980).
[12] M. E. Brachet, D. I. Meiron, S. A. Orszag, B. G. Nickel, R. H. Morf, and U. Frisch, J. Fluid. Mech. **130**, 441 (1983).
[13] M. E. Brachet, M. Meneguzzi, A. Vincent, H. Politano, and P. L. Sulem, Phys. Fluids **4**, 2845 (1992).
[14] S. Kida, J. Phys. Soc. Jpn. **54**, 2132 (1985).
[15] J. A. M. Vermaseren, FORM (Computer Algebra Netherland, Amsterdam, 1991).
[16] T. Granlund, GMP, 1996, now available by anonymous ftp from sics.se.
[17] D. H. Bailey, RNR Technical Report No. RNR-90-022, 1993.
[18] B. Salvy and Paul Zimmerman, ACM Trans. on Math. Softw. **20**, 163 (1994).
[19] O. N. Boratav and R. B. Pelz (unpublished).
[20] R. M. Kerr, Phys Fluids A **5**, 1725 (1993).